# *Supplementary Material*

## 1 Particle size distribution and shape characteristics

Particle size distributions (Supplementary Figure 1) and shape characteristics of MP particles were obtained by static image analysis (International Organization for Standardization 2014) using a stereomicroscope with a camera (Leica MZ16 FA & Leica DFC420 C, Leica Microsystems, Heerbrugg, Switzerland). Images were processed with a customized macro in image analysis software Fiji 1.52p (Schindelin et al. 2012; Schneider et al. 2012) including a thresholding procedure based on Brocher (2014). Particles were then measured with the morphology plugin by Landini (2008). According to Shekunov et al. (2007), data entries with a Feret's diameter $\leq 3$ µm were completely removed due to the measurement range of light microscopes using R software (R Core Team 2018). In addition, particles > 99.7% percentile were excluded as they showed heavy agglomeration. In this way, a total of 8.51% (LDPE) and 7.47% (PLA/PBAT) of data entries were filtered out. Values of circularity and elongation were removed when they exceeded the maximum values of the theoretical model as proposed by Kröner and Doménech Carbó (2013). Finally, shape characteristics (elongation, circularity, and convexity) were calculated as described in Crompton (2005).

Particles of LDPE and PLA/PBAT were characterized as irregularly shaped based on a circularity of $0.53 \pm 0.15$ and $0.57 \pm 0.16$, elongation of $0.36 \pm 0.16$, $0.34 \pm 0.16$, and convexity of $0.84 \pm 0.09$ and $0.86 \pm 0.09$, respectively (Supplementary Figure 1).

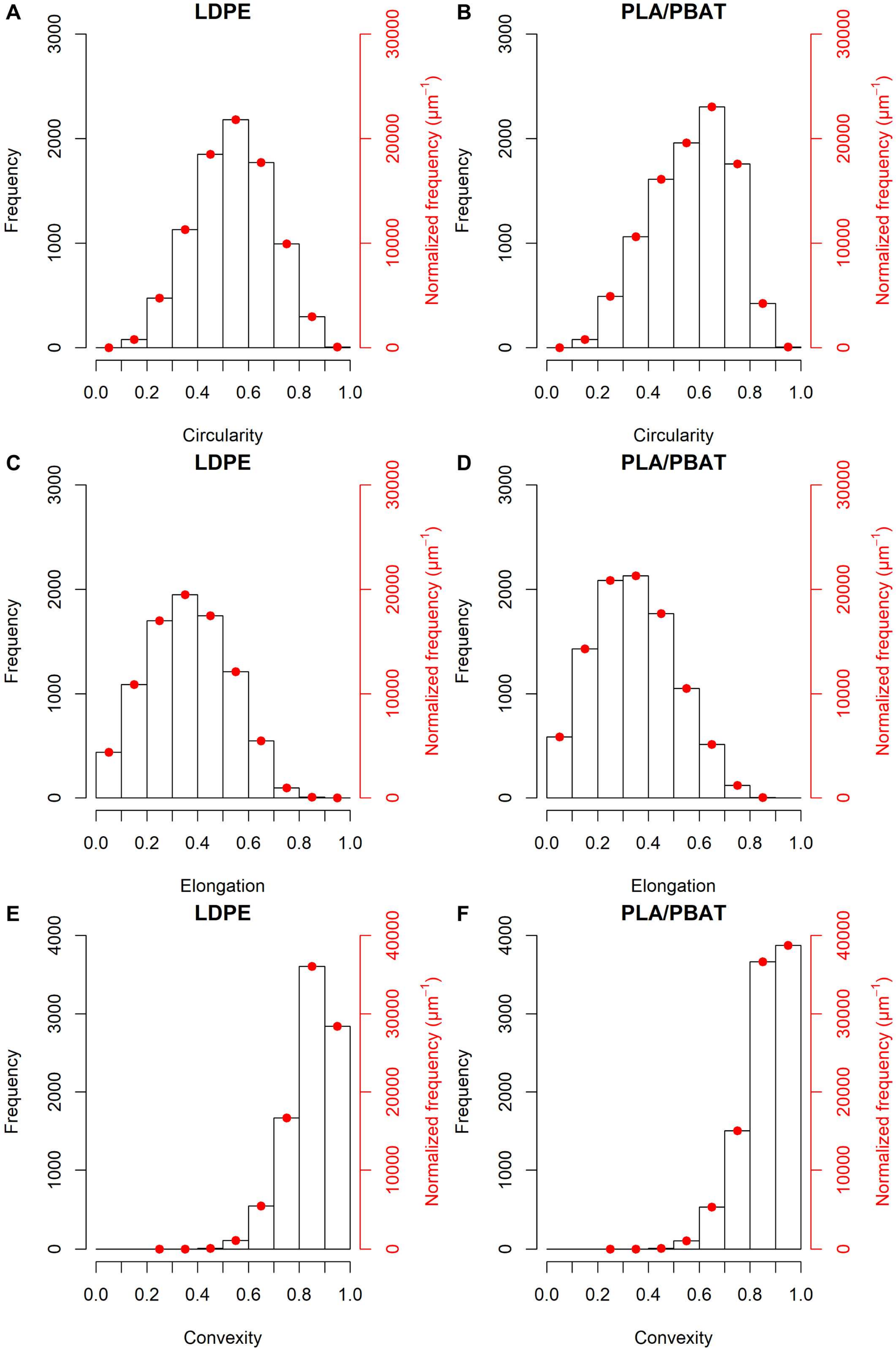

A
LDPE
Frequency
Normalized frequency (µm⁻¹)
Circularity
B
PLA/PBAT
Frequency
Normalized frequency (µm⁻¹)
Circularity
C
LDPE
Frequency
Normalized frequency (µm⁻¹)
Elongation
D
PLA/PBAT
Frequency
Normalized frequency (µm⁻¹)
Elongation
E
LDPE
Frequency
Normalized frequency (µm⁻¹)
Convexity
F
PLA/PBAT
Frequency
Normalized frequency (µm⁻¹)
Convexity

**Supplementary Figure 1.** Shape characteristics of LDPE (n = 8790) and PLA/PBAT (n = 9694) particles. Circularity, elongation, and convexity of LDPE (A, C, E) and PLA/PBAT (B, D, F) respectively. Three entries per plastic type were removed by the Kröner and Doménech Carbó (2013) algorithm. Circularity measures how much a particle deviates from a perfect circle. Values closer to one indicate a spherical shape, while values closer to zero are typical for fibers and irregularly shaped particles. Elongation measures the aspect ratio ration of particles. Values closer to one indicate a very small width-to-length ration, while values closer to zero are typical for particles with a circular or rectangular surface. Note that particles with both a rough and a smooth surface might have equal elongations. Convexity measures the surface roughness of particles. Values close to one will be found in case of smooth surfaces, while values closer to zero are typical for irregularly shaped particles. Note that one cannot differentiate between fibers and spheres when both have the same convexity.

**Supplementary Table 1.** Experimental design of reproduction and body length assay with number of replicates (n) used in the statistical analysis, means, standard errors (SE), and coefficients of variation (CV).

| | | Offspring | | | | Body length | | | |
|---|---|---|---|---|---|---|---|---|---|
| Plastic type | Concentration level (mg $L^{-1}$) | n | Mean | SE | CV (%) | n | Mean (µm) | SE (µm) | CV (%) |
| Control | 0 | 6 | 267 | 6.0 | 5.5 | 6 | 1470 | 24.3 | 4.1 |
| LDPE | 1 | 6 | 255 | 15.1 | 14.5 | 6 | 1354 | 25.9 | 4.7 |
| | 10 | 6 | 206 | 11.1 | 13.2 | 6 | 1340 | 58.0 | 10.6 |
| | 100 | 5 | 229 | 9.4 | 9.2 | 5 | 1488 | 36.0 | 5.4 |
| PLA/PBAT | 1 | 7 | 250 | 16.1 | 17.0 | 7 | 1256 | 67.2 | 14.2 |
| | 10 | 5 | 237 | 17.5 | 16.5 | 5 | 1457 | 75.9 | 11.6 |
| | 100 | 6 | 232 | 9.9 | 10.5 | 5 | 1410 | 44.0 | 7.0 |

**Supplementary Table 2.** Specified comparisons of means between the treatments of reproduction and body length assay with difference and [lower; higher] 95% confidence interval including p value. LDPE: low-density-polyethylene. PLA/PBAT: blend of biodegradable polymers polylactide (PLA) and poly(butylene adipate-co-terephthalate) (PBAT). Indices denote the concentration levels of 0, 1, 10 and 100 mg $L^{-1}$.

| | Offspring | | Body length | |
|---|---|---|---|---|
| Comparison between treatments | Difference | p value | Difference (µm) | p value |
| $LDPE_1$ vs. $Control_0$ | -12 [-67; +43] | 0.63 | -115 [-333; +103] | 0.25 |
| $LDPE_{10}$ vs. $Control_0$ | -61 [-116; -6] | 0.03 | -129 [-347; +89] | 0.21 |
| $LDPE_{100}$ vs. $Control_0$ | -39 [-96; +19] | 0.23 | +18 [-210; +247] | 0.86 |
| $PLA/PBAT_1$ vs. $Control_0$ | -18 [-71; +35] | 0.49 | -213 [-423; -3] | 0.06 |
| $PLA/PBAT_{10}$ vs. $Control_0$ | -30 [-88; +27] | 0.30 | -13 [-242; +216] | 0.86 |
| $PLA/PBAT_{100}$ vs. $Control_0$ | -35 [-90; +20] | 0.23 | -60 [-289; +169] | 0.59 |
| $LDPE_{10}$ vs. $LDPE_1$ | -49 [-104; +6] | 0.08 | -14 [-232; +204] | 0.86 |
| $LDPE_{100}$ vs. $LDPE_{10}$ | +23 [-35; +80] | 0.44 | +147 [-81; +376] | 0.21 |
| $LDPE_{100}$ vs. $LDPE_1$ | -26 [-84; +31] | 0.37 | +133 [-95; +362] | 0.21 |
| $PLA/PBAT_{10}$ vs. $PLA/PBAT_1$ | -13 [-68; +43] | 0.63 | +200 [-21; +422] | 0.07 |
| $PLA/PBAT_{100}$ vs. $PLA/PBAT_{10}$ | -5 [-62; +53] | 0.85 | -47 [-286; +192] | 0.69 |
| $PLA/PBAT_{100}$ vs. $PLA/PBAT_1$ | -17 [-70; +36] | 0.49 | +153 [-68; +375] | 0.21 |
| $LDPE_1$ vs. $PLA/PBAT_1$ | +6 [-47; +59] | 0.85 | +98 [-112; +308] | 0.27 |
| $LDPE_{10}$ vs. $PLA/PBAT_{10}$ | -31 [-89; +27] | 0.30 | -116 [-345; +112] | 0.25 |
| $LDPE_{100}$ vs. $PLA/PBAT_{100}$ | -4 [-61; +54] | 0.85 | +78 [-161; +317] | 0.49 |

## 2 References


Brocher, J. (2014). Qualitative and quantitative evaluation of two new histogram limiting binarization algorithms. *International Journal of Image Processing (IJIP)* 8, 30–48.

Crompton, C. (2005). Particle shape: An important parameter in pharmaceutical manufacturing. *Pharmaceutical Manufacturing and Packing Sourcer*.

International Organization for Standardization (2014). ISO 13322-1:2014: Particle size analysis - image analysis methods - part 1: Static image analysis methods.

Kröner, S., and Doménech Carbó, M. T. (2013). Determination of minimum pixel resolution for shape analysis: Proposal of a new data validation method for computerized images. *Powder Technology* 245, 297–313. doi:10.1016/j.powtec.2013.04.048.

Landini, G. (2008). "Advanced shape analysis with imagej," in *Proceedings of the second imagej user and developer conference* (Luxembourg), 116–121.

R Core Team (2018). R: A language and environment for statistical computing. Available at: https://www.R-project.org/.

Schindelin, J., Arganda-Carreras, I., Frise, E., Kaynig, V., Longair, M., Pietzsch, T., et al. (2012). Fiji: An open-source platform for biological-image analysis. *Nature methods* 9, 676–682. doi:10.1038/nmeth.2019.

Schneider, C. A., Rasband, W. S., and Eliceiri, K. W. (2012). NIH image to ImageJ: 25 years of image analysis. *Nature methods* 9, 671–675.

Shekunov, B. Y., Chattopadhyay, P., Tong, H. H. Y., and Chow, A. H. L. (2007). Particle size analysis in pharmaceutics: Principles, methods and applications. *Pharmaceutical research* 24, 203–227. doi:10.1007/s11095-006-9146-7.